

Assessing Potential Supports for Lithium Amide-imide Ammonia Decomposition Catalysts

Thomas J. Wood^{†*} and Joshua W. Makepeace[‡]

[†] ISIS Facility, Rutherford Appleton Laboratory, Didcot, OX11 0QX, UK

[‡] Inorganic Chemistry Laboratory, University of Oxford, Oxford, OX1 3QR, UK

*Corresponding author: thomas.wood@stfc.ac.uk

Keywords: ammonia decomposition; catalyst; supports; lithium amide; lithium imide.

ABSTRACT

Lithium amide-imide is an excellent ammonia decomposition catalyst, but its highly reactive nature makes the application of traditional heterogeneous catalyst methods challenging, including the use of porous supports. In this study, lithium amide-imide was tested for compatibility with various support materials (activated carbon, silicon dioxide, aluminium oxide and magnesium oxide). It was found that most of the supports were unsuitable due to their reactivity with the catalyst, especially under flowing ammonia at decomposition conditions (>400 °C and 1 bar). Magnesium oxide, however, did not react with lithium amide-imide under flowing ammonia. Ammonia decomposition experiments over these catalyst-support mixtures showed that the lithium amide-imide/magnesium oxide system gave the best performance and therefore represents an excellent and usable ammonia decomposition catalyst.

INTRODUCTION

Ammonia has recently garnered renewed interest as an energy vector^{1,2,3} because of promising properties such as: (i) having around 40% the specific energy of octane, but releasing only nitrogen gas and water on combustion; (ii) being liquid at 10 bar and room temperature thus making it straightforward to store; (iii) having already a large infrastructure given its current worldwide production on the 100 megatonne scale (mostly for use as fertilizer feedstock⁴). One of the major hurdles facing adoption of an ammonia economy, however, is that for energy release, the ammonia needs to be decomposed to release hydrogen (and nitrogen) gas—fully in the case of fuel cells^{5,6} and partially in the case of internal combustion engines⁷ (in order to improve flame propagation and flammability window properties).

Traditional, state-of-the-art ammonia decomposition catalysts are based on transition metals with ruthenium offering the highest activity.^{8,9,10} The limitations of ruthenium, however, are its cost and (closely linked) the fact that there are limited ruthenium resources worldwide (around 1 ppb in the earth's crust).¹¹ Other transition metal catalysts are iron and nickel, which make up for their poorer performance compared to ruthenium by their vastly decreased costs and increased natural

abundance.^{3,12} Recently it was found that a variety of alkali (and alkaline earth) metal amides or imides are also catalytically active with regard to ammonia decomposition. These included sodium amide,¹³ lithium amide-imide,^{14,15,16} lithium calcium imide¹⁷ and calcium imide.¹⁸ Of these, the sodium amide catalyst, while giving catalytic performances close to ruthenium, is liquid at ammonia decomposition temperatures (>400 °C), which leads to significant catalyst loss.^{13,19} Lithium amide-imide ($\text{Li}_{2-x}\text{NH}_{1+x}$), however, remains solid, as long as the catalyst solid solution remains sufficiently towards the lithium imide end (i.e. x is small).¹⁵ The solid nature of the catalyst in the lithium amide-imide system means that catalyst escape is minimized and more traditional strategies for maximising catalyst performance can be employed. One such strategy is supporting the catalyst on another material which can increase catalyst surface area or even interact with the catalyst through a variety of promotion mechanisms in order to increase the catalyst's turnover frequency. In the case of metal amide catalysts, however, since it is known that the entire catalyst (not just isolated surface sites) is chemically active during ammonia decomposition,^{15,19,20} an inert (or synergetic) support would also ensure that gas flow is easily maintained through a catalyst bed by hindering sintering and catalyst movement. The fact that the bulk material is intimately involved in the catalytic reaction is a fundamental difference between metal amide catalysts and traditional, supported metal nanoparticle catalysts, and, as a result the nature of the bulk and the surface of the former are constantly changing (dependent on conditions) during ammonia decomposition (as evidenced by in-situ powder diffraction and mass spectrometry studies^{15,20}).

In this study, lithium amide-imide was chosen as the metal amide/imide to decompose ammonia, since it forms a solid solution ($\text{Li}_{2-x}\text{NH}_{1+x}$)^{15,21,22} and therefore is a useful test case for catalyst-support interactions for both metal amides and imides. Four support materials (activated charcoal, silicon dioxide, γ -aluminium oxide and magnesium oxide) were studied with regards to their stability with lithium imide and lithium amide under inert gas (argon) as well as lithium amide under ammonia.

EXPERIMENTAL

Materials used in this work were: lithium amide (95%, Sigma-Aldrich), activated charcoal (100–400 mesh, Sigma-Aldrich), silicon dioxide (99.9%, Aldrich), γ -aluminium oxide (1/8" pellets ground, Alfa Aesar) and magnesium oxide ($\geq 98.0\%$, Fluka). The activated charcoal, silicon dioxide, aluminium oxide and magnesium oxide were all dried (separately) by heating to 550 °C for >12 h under flowing argon. Lithium imide was synthesised by the solid state reaction between lithium amide and lithium nitride (~ 80 mesh, $\geq 99.5\%$, Aldrich), $\text{Li}_3\text{N}_{(s)} + \text{LiNH}_{2(s)} \rightarrow 2\text{Li}_2\text{NH}_{(s)}$, which comprised grinding equimolar amounts and heating to 300 °C for 12 h under a low flow of argon.

Simultaneous thermal analysis (combined thermogravimetric analysis [TGA] and differential scanning calorimetry [DSC]) measurements were performed on a Netzsch F3 Jupiter machine. Samples were prepared by hand grinding 0.1 g of lithium amide or lithium imide with 0.1 g of one of activated charcoal, silicon dioxide, aluminium oxide or magnesium oxide in an argon-filled glovebox. Approximately 8 mg of each mixture was placed into an aluminium pan and sealed. The lid was then punctured before placing into the STA furnace in order to let any gases emitted during heating to escape. Samples were heated to 580 °C under flowing argon. No measurements were taken under flowing ammonia, because the reactants tend to escape the container, thus hindering any useful data collection.

Reactions between 0.1 g lithium imide or lithium amide mixed with 0.1 g of one of activated charcoal, silicon dioxide, aluminium oxide or magnesium oxide were performed in a stainless steel reactor (47 cm³ internal volume) fitted with an inlet pipe that directed gas in to just above the sample surface.¹³ The sample mixtures were hand ground together in an agate pestle and mortar within an argon-filled glovebox prior to loading into the reactor. The reactor was then attached to a gas panel with a mass spectrometer (Hiden Analytical HPR-20 QIC R&D) employed to analyse the exhaust gases (m/z histograms were taken for the range 1–40). Flowing argon or ammonia was mediated through a mass flow controller (HFC302, Teledyne-Hastings Ltd.) and the outlet gas flow was measured by a mass flow meter (HFM300, Teledyne-Hastings Ltd.). Twelve mixtures were reacted to 520 °C (at 3.6 °C min⁻¹) comprising each of activated charcoal, silicon dioxide, aluminium oxide and magnesium oxide heated with (i) lithium imide under argon, (ii) lithium amide under argon and (iii) lithium amide under ammonia.

X-ray powder diffraction patterns of the twelve samples that had been thus reacted were taken in the Debye-Scherrer configuration using a Rigaku Smartlab Diffractometer equipped with a copper source (1.542 Å) and a germanium monochromator. Samples were loaded into 0.7 mm borosilicate capillaries in an argon-filled glovebox before being attached to the diffractometer. The capillaries were rotated during measurements in order to eliminate preferred orientation effects. The collected diffraction patterns were analysed with the Rietveld method using TOPAS v5 (Bruker APS).

Ammonia decomposition behaviour was measured using the aforementioned stainless steel reactor with mass spectrometer setup. For each reaction, 0.5 g of lithium amide was hand-ground in an agate mortar and pestle with 0.5 g of one of activated charcoal, silicon dioxide, aluminium oxide or magnesium oxide before being placed into the reactor and subjected to 30 cm³ min⁻¹ NH₃ flow. The reactor was heated to 10 different temperatures between 325 °C and 525 °C and was allowed to

equilibrate for 2 h at each temperature before the extent of NH_3 decomposition was recorded. The data thus collected were fitted to a Gompertz sigmoid function.¹³

RESULTS

Carbon

The reaction of Li_2NH with activated charcoal (carbon) showed a broad endothermic feature at $\sim 375^\circ\text{C}$, which coincided with a small mass loss (1.5%) and a release of H_2 in the mass spectrometry data, Figure 1(a). Lithium imide by itself only begins to decompose at temperatures above 600°C to Li_4NH with concomitant release of equimolar amounts N_2 and H_2 , although a small release of H_2 may be seen above 400°C (Figure S1).^{23,24} Similarly, in the case of LiNH_2 with carbon, there is a broad endotherm at the same point, but a larger mass loss and a sharp endotherm at 370°C relating to the melting of LiNH_2 . The release of ammonia seen in the mass spectrometry trace (Figure 1(c)(ii)) indicates that the LiNH_2 has begun to decompose to Li_2NH before reacting with the carbon. LiNH_2 by itself decomposes to Li_2NH (endothermically) with release of NH_3 at an onset temperature of around 300°C under inert gas (see Figure S2),^{23,25} whereas under flowing NH_3 the mass spectrometry signal is dominated by decomposition of NH_3 to N_2 and H_2 from 400°C (with a small prior H_2 release associated with surface nitriding of the reactor walls, see Figure S3²⁰). Both reactions under argon and the reaction of LiNH_2 with carbon under NH_3 form a majority phase of Li_2NCN (see Figure 2), which is not as active as an ammonia decomposition catalyst as the original lithium amide-imide.²⁶ Therefore activated carbon is not an appropriate support for either lithium amide or lithium imide ammonia decomposition catalysts.

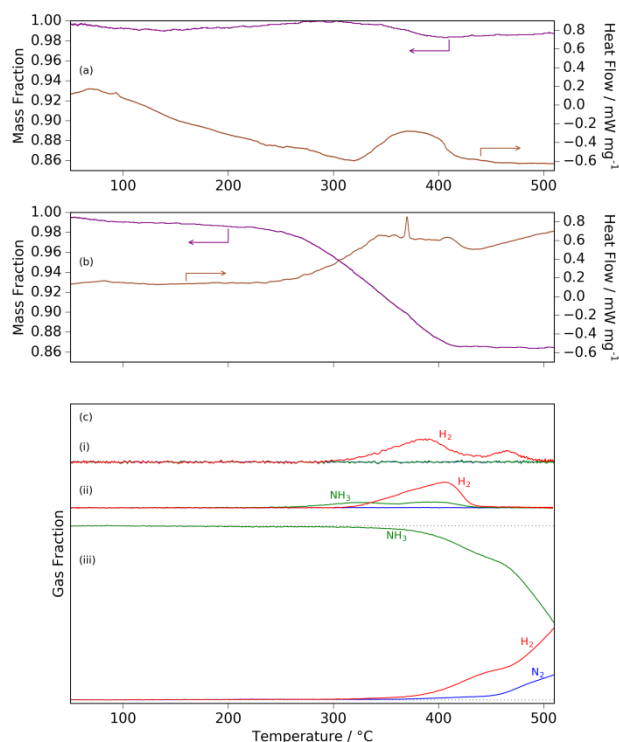


Figure 1: (a) TGA and DSC traces for $\text{Li}_2\text{NH}/\text{C}$ under Ar; (b) TGA and DSC traces for LiNH_2/C under Ar; (c) mass spectrometry data for (i) $\text{Li}_2\text{NH}/\text{C}$ under Ar, (ii) LiNH_2/C under Ar, (iii) LiNH_2/C under NH_3 . The mass spectrometry traces omit Ar and normalize (i) and (ii) to 15% of (iii) for clarity.

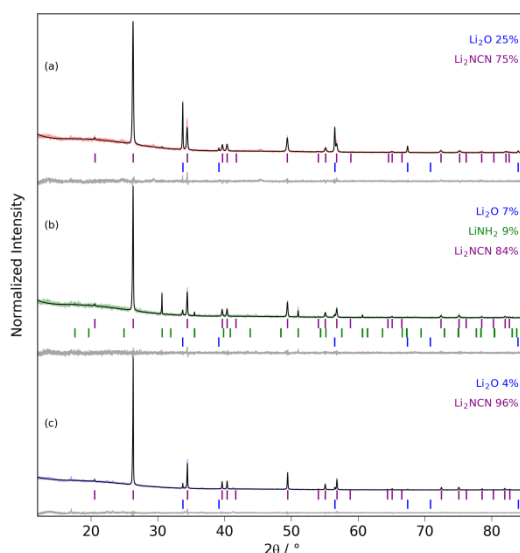


Figure 2: XRD patterns for: (a) the products of Li_2NH and activated charcoal (carbon) heated under Ar; (b) LiNH_2 and carbon heated under Ar; (c) LiNH_2 and carbon heated under NH_3 .

Silicon dioxide

The reaction of Li_2NH with SiO_2 under flowing argon showed a small sample mass loss pertaining to hydrogen loss in the sample, Figure 3(a) and (c)(i). The DSC trace only showed small endothermic peaks

below 100 °C, which are associated with a disordering of the lithium imide from a $Fd\bar{3}m$ to a $Fm\bar{3}m$ structure.²⁷ This is consistent with the X-ray diffraction pattern, which shows that the majority of the sample stayed as Li_2NH with only a small amount of oxidation to Li_2O , Figure 4(a). This small amount of oxidation is presumed to be the reason behind the small mass loss ($\sim 1\%$) and release of H_2 seen in the mass spectrometry data (Figure 3(a) and (c)(i) respectively), albeit a very small amount of H_2 was also released for Li_2NH by itself at a similar temperature (see Figure S1). In contrast to the reaction of Li_2NH with SiO_2 under Ar, when Li_2NH is replaced with LiNH_2 , there was a steady mass loss from 125 °C to 340 °C ($\sim 3.5\%$), whereupon there was a more significant decrease in the sample mass fraction to 0.81, Figure 3(b). This mass loss was concurrent with a broad endotherm in the DSC trace, which also featured a sharp endotherm at 370 °C related to the melting of LiNH_2 . The mass spectrometry traces for this reaction showed a release of hydrogen and ammonia over this period, which was consistent with the XRD data revealing the majority of the LiNH_2 had reacted to become Li_2O , Figure 4(b). This difference in extent of reaction between Li_2NH and LiNH_2 (to form Li_2O) can be attributed to the latter's lower melting point, which enables better contact between the amide and the SiO_2 .

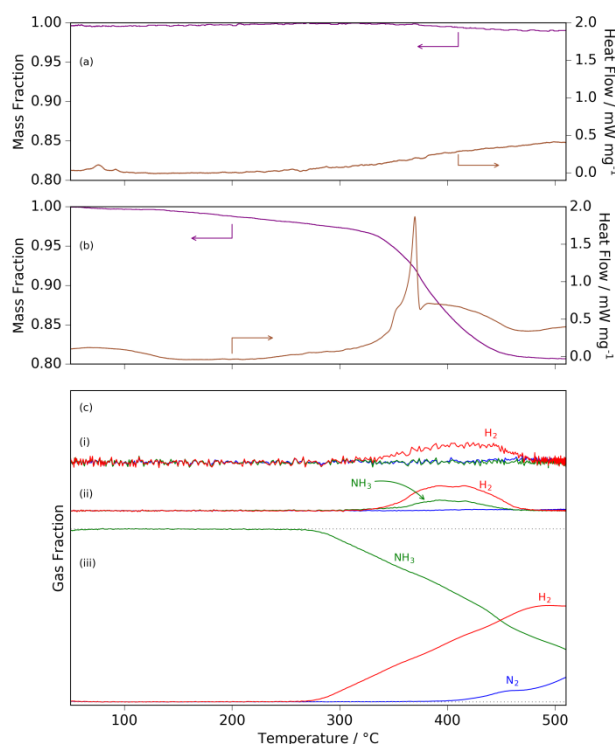


Figure 3: (a) TGA and DSC traces for $\text{Li}_2\text{NH}/\text{SiO}_2$ under Ar; (b) TGA and DSC traces for $\text{LiNH}_2/\text{SiO}_2$ under Ar; (c) mass spectrometry data for (i) lithium imide/silicon dioxide under Ar, (ii) $\text{LiNH}_2/\text{SiO}_2$ under Ar, (iii) $\text{LiNH}_2/\text{SiO}_2$ under NH_3 . The mass spectrometry traces omit Ar and normalize (i) and (ii) to 15% of (iii) for clarity.

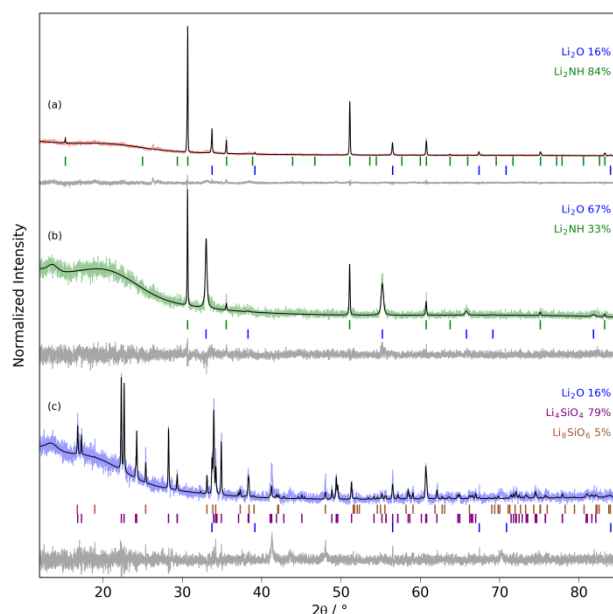


Figure 4: XRD patterns for: (a) the products of Li_2NH and SiO_2 heated under Ar; (b) LiNH_2 and SiO_2 heated under Ar; (c) LiNH_2 and SiO_2 heated under NH_3 .

The reactions between Li_2NH or LiNH_2 and SiO_2 under argon might lead to the conclusion that with ammonia decomposition reactions, if the $\text{Li}_{2-x}\text{NH}_{1+x}$ solid solution can be kept as a solid (i.e. when x is small and the structure is closer to the imide), then SiO_2 could be a usable support. The reaction between LiNH_2 and SiO_2 under flowing NH_3 , however, showed a marked difference in the products obtained with small fractions of Li_8SiO_6 and Li_2O (5 wt% and 16 wt% respectively) but a majority phase of Li_4SiO_4 , Figure 4(c); there was no Li_2NH or LiNH_2 observed. The mass spectrometry data from this reaction showed a significant release of H_2 from 280 °C as well as a small release of N_2 at 460 °C (NH_3 decomposition accounts for part of the H_2 and N_2 signals from 400 °C), which indicates that the reaction had at least two steps and started from ~275 °C. This is analogous to the observed reaction between sodium amide and silicon dioxide which resulted in sodium silicates forming.²⁸ The reaction between LiNH_2 and SiO_2 under the same conditions as when NH_3 decomposition would be expected to occur means that SiO_2 is an inappropriate catalyst support for the $\text{Li}_{2-x}\text{NH}_{1+x}$ system.

Aluminium Oxide

The TGA trace for the reaction between Li_2NH and Al_2O_3 under Ar showed a small mass loss (~2%) until ~330 °C when the mass loss rate increased to give a final mass fraction of 0.89, Figure 5(a). The DSC trace showed a small, broad exotherm at around 330 °C followed by a smaller endotherm at 370 °C, which could be associated with the mass loss; the mass spectrometry trace showed H_2 release at the same temperature as the mass loss. The XRD pattern for the $\text{Li}_2\text{NH}/\text{Al}_2\text{O}_3$ reaction showed that there was no Li_2NH left with only Li_2O and $\gamma\text{-Al}_2\text{O}_3$ products (see Figure 6(a)), which is consistent with the

large mass loss. The broad peaks of the Li_2O phase relate to a small crystallite size of 12(2) nm as well as some strain effects. There was a similar reaction for the $\text{LiNH}_2/\text{Al}_2\text{O}_3$ case, with a large mass loss and small, broad endotherm (Figure 5(b), again the sharp endotherm at 372 °C was the LiNH_2 melting) leading to reaction products of Li_2O and $\gamma\text{-Al}_2\text{O}_3$ (with a very small amount of Li_2NH), Figure 6(b). Again, the broad peaks of Li_2O relate to small crystallite sizes of 13(4) nm. Given the contrast with the sharpness of the Li_2NH phase peaks, it is reasonable to suppose that reaction with the small particles of $\gamma\text{-Al}_2\text{O}_3$ is responsible for this effect. The mass spectrometry traces for this reaction showed release of NH_3 from 210 °C, which is attributed to the decomposition of LiNH_2 into Li_2NH ($2\text{LiNH}_2 \rightarrow \text{Li}_2\text{NH} + \text{NH}_3$). The LiNH_2 reaction, therefore, probably proceeds via Li_2NH .

When LiNH_2 is reacted with Al_2O_3 under NH_3 , the only products were LiAlO_2 and Li_5AlO_4 (Figure 6(c)); this latter phase formed in two orthorhombic polymorphs. Similar to the reactions with SiO_2 , it seems that the presence of gaseous ammonia suppresses Li_2O formation and instead promotes the production of lithium silicates or lithium aluminates. These reactions render Al_2O_3 also inappropriate as a support for the $\text{Li}_{2-x}\text{NH}_{1+x}$ catalyst under ammonia decomposition conditions.

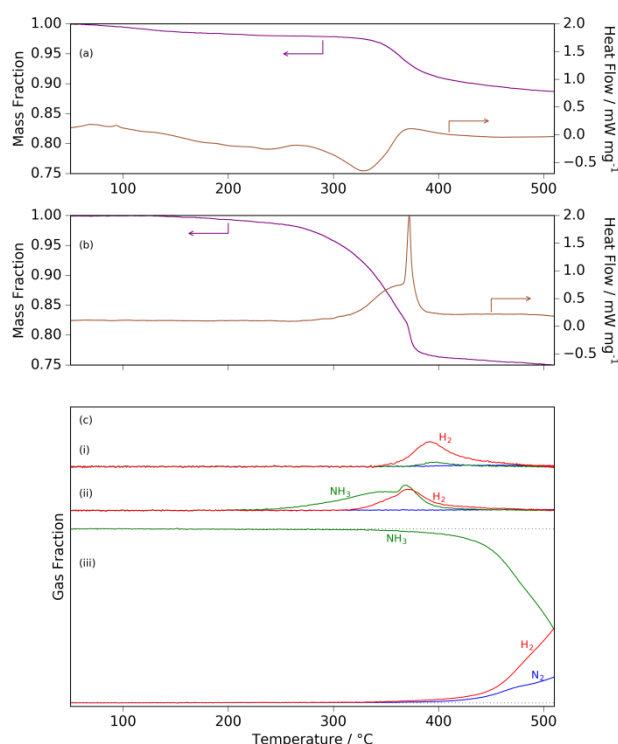


Figure 5: (a) TGA and DSC traces for $\text{Li}_2\text{NH}/\text{Al}_2\text{O}_3$ under Ar; (b) TGA and DSC traces for $\text{LiNH}_2/\text{Al}_2\text{O}_3$ under Ar; (c) mass spectrometry data for (i) $\text{Li}_2\text{NH}/\text{Al}_2\text{O}_3$ under Ar, (ii) $\text{LiNH}_2/\text{Al}_2\text{O}_3$ under Ar, (iii) $\text{LiNH}_2/\text{Al}_2\text{O}_3$ under NH_3 . The mass spectrometry traces omit Ar and normalize (i) and (ii) to 15% of (iii) for clarity.

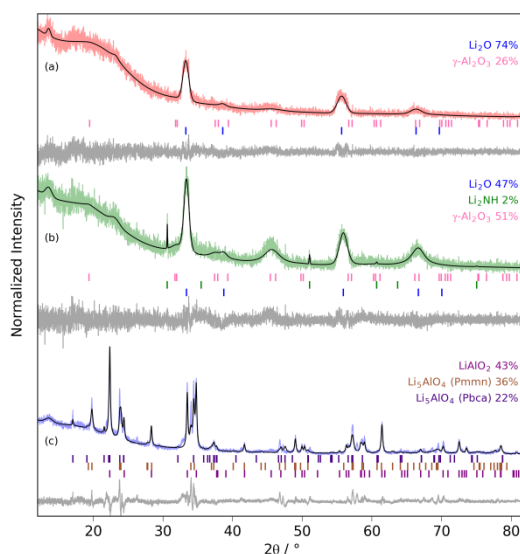


Figure 6: XRD patterns for: (a) the products of Li_2NH and Al_2O_3 heated under Ar; (b) LiNH_2 and Al_2O_3 heated under Ar; (c) LiNH_2 and Al_2O_3 heated under NH_3 .

Magnesium oxide

The final support material to be assessed was magnesium oxide (MgO). The TGA trace for the reaction between MgO and Li_2NH showed a small mass decrease (around 3%) starting at $\sim 380^\circ\text{C}$, Figure 7(a). As seen before for SiO_2 , Al_2O_3 and carbon, this mass decrease corresponded to a release of H_2 in the mass spectrometry data for the reaction and the XRD patterns showed a significant proportion of Li_2O (as well as unreacted MgO), (see Figure 7(c)(i) and Figure 8(a) respectively). Rietveld analysis of the XRD pattern revealed that the ternary nitride, LiMgN in two crystal settings (face-centred cubic and primitive orthorhombic) comprised around 43 wt% of the final products. These phases were also observed in the reaction between LiNH_2 and MgO , albeit at a significantly lower proportion (see Figure 8(b)). Li_2O and unreacted MgO were also present in this case and the mass spectrometry traces showed that NH_3 was once again released from the LiNH_2 , which is a hallmark of decomposition into Li_2NH (Figure 7(c)(ii)). This is confirmed on inspection of the TGA trace which showed a small initial mass loss at lower temperatures followed by a larger mass loss (sample mass fraction decreased to 0.81) at 370°C , which coincided with both a broad endotherm and the sharper endotherm associated with LiNH_2 melting, Figure 7(b).

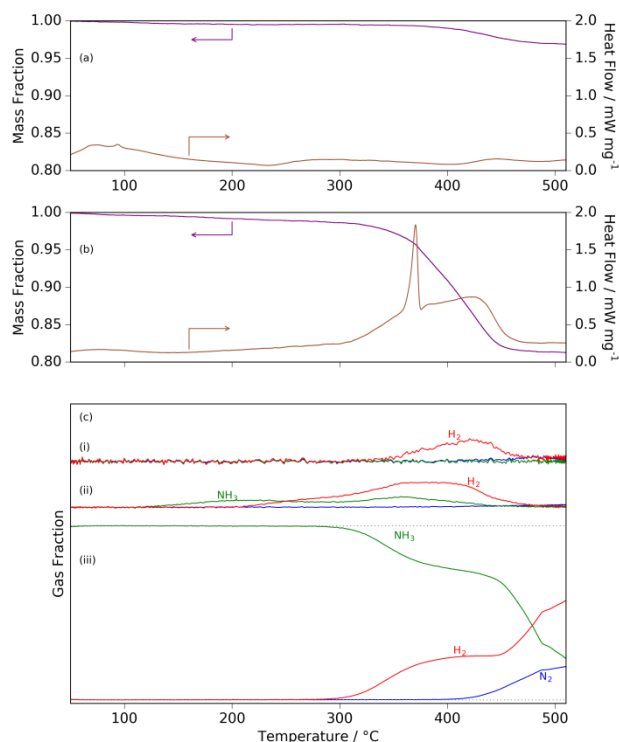


Figure 7: (a) TGA and DSC traces for $\text{Li}_2\text{NH}/\text{MgO}$ under Ar; (b) TGA and DSC traces for LiNH_2/MgO under Ar; (c) mass spectrometry data for (i) $\text{Li}_2\text{NH}/\text{MgO}$ under Ar, (ii) LiNH_2/MgO under Ar, (iii) LiNH_2/MgO under NH_3 . The mass spectrometry traces omit Ar and normalize (i) and (ii) to 15% of (iii) for clarity.

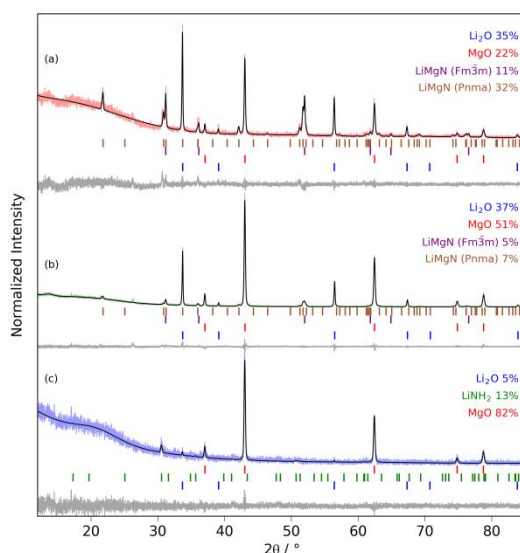


Figure 8: XRD patterns for: (a) the products of Li_2NH and MgO heated under Ar; (b) LiNH_2 and MgO heated under Ar; (c) LiNH_2 and MgO heated under NH_3 .

The mass spectrometry traces of the reaction of LiNH_2 and MgO under flowing NH_3 showed a release of H_2 from ~300 °C, which implies that some the LiNH_2 has reacted, Figure 7(c)(iii). However, the XRD pattern for the products indicated that there were significant proportions of unreacted LiNH_2 and MgO

(13(2) wt % and 82(2) wt % respectively) along with small amounts of Li_2O . This could be a result of the ternary nitride, LiMgN , forming (as in the reactions under Ar) at lower temperatures followed by its reaction with NH_3 to reform LiNH_2 (in a reaction analogous to that of the lithium iron nitride, Li_3FeN_2 ²⁹); in this scenario, formation of Li_2NH and therefore Li_2O would be avoided. The consequence of these reactions is that the LiNH_2 catalyst is available to decompose ammonia when mixed with MgO support.

Ammonia decomposition

The expectation from the above reactions that MgO is likely to be the best of the potential supports for $\text{Li}_{2-x}\text{NH}_{1+x}$ was confirmed by testing the ammonia conversion of the different lithium amide/support mixtures. It can be seen that the performance of LiNH_2 on its own is approximately the same as LiNH_2 with MgO , Figure 9. Lithium amide mixed with activated charcoal showed no ammonia decomposition activity above the background of the stainless steel reactor and lithium amide mixed with aluminium oxide had a significantly reduced catalytic ability. Lithium amide mixed with silicon dioxide shadowed the catalytic performance of unadulterated lithium amide up to around conversion of 0.5, but then significantly tailed off.

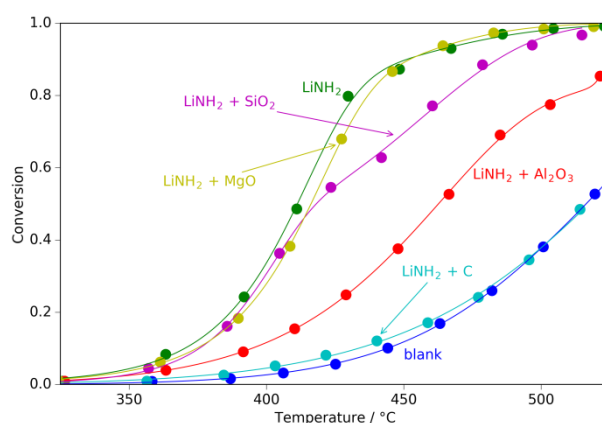


Figure 9: Plot of conversion of ammonia to nitrogen and hydrogen for lithium amide as well as lithium amide mixtures with activated charcoal, silicon dioxide, aluminium oxide and magnesium oxide.

DISCUSSION

Alkali or alkaline earth metal amides and imides represent a new class of ammonia decomposition catalysts characterized by high activities and low costs. In order to maximise their effectiveness, however, these catalysts need to be: (i) contained within the reaction vessel; (ii) present the maximum number of active sites to the reactant (i.e. high surface area); (iii) allow gas flow through the catalyst bed. Supports (inert or otherwise) can help with all of these aims, but, since these catalysts are based on earth-abundant (and therefore inexpensive) elements, catalyst containment and allowing gas flow

through the catalyst bed are the most important considerations. Indeed this latter consideration is particularly important in this class of catalysts since it has been well established that the bulk of the catalyst material reacts (to form a non-stoichiometric solid solution between the lithium amide and imide end members) over the course of ammonia decomposition (depending on the exact conditions).¹⁵ An ideal support material would be chemically inert to the catalyst (or even promote the reaction being catalysed) as well as having good thermal conductivity and high surface area.

As evidenced by the results for activated carbon, silicon dioxide, aluminium oxide and magnesium oxide, lack of chemical reactivity of the support to the lithium amide-imide catalyst is not straightforwardly achieved. All of the supports studied here are used in many catalytic reactions precisely because of their lack of reactivity or their high surface area. Alkali or alkaline earth metal amides ($M^+NH_2^-$) are very strong Brønsted bases, however, and the imide anion (NH_2^- , having lost another proton) is even stronger. This strong basicity means that it is difficult to find chemically unreactive supports. This is evidenced by their reactions with activated carbon to form the lithium carbodiimide species Li_2NCN , rendering carbon an unsuitable support material despite its high surface area. In general, one would expect lithium imide to be more reactive than lithium amide and this is borne out by the relative enthalpies of formation (-222 kJ mol^{-1} and -176 kJ mol^{-1} respectively³⁰), where double the stoichiometric ratio of amide is required to give the same amount of lithium oxide (or other lithium-containing) product; however, any unreacted lithium amide will decompose to lithium imide at temperatures below 400°C (when ammonia is decomposed). Given their basicity, the most obvious candidate for a support material would be one that is itself basic (or at least not acidic or amphoteric). The oxide supports in this study are all oxides of period 3 elements, where, as we move across the period from magnesium, through aluminium and to silicon, the acid-base behaviour follows the trend to greater acidity/less basicity. The result of this is that magnesium oxide is basic, aluminium oxide is amphoteric and silicon dioxide is weakly acidic.

Given these properties, it is unsurprising that lithium amide reacts with silicon dioxide under argon to form lithium oxide. The increase in extent of reaction with lithium amide and silicon dioxide compared to lithium imide (where very little reaction is observed) can be explained by the melting of the lithium amide increasing the reactive surface area. Similarly, for aluminium oxide the reactions with both lithium imide and lithium amide under argon form lithium oxide. For both silicon dioxide and aluminium oxide the reaction under ammonia yields ternary oxides with both lithium and silicon or aluminium. Clearly, in both these cases, both the lithium amide and lithium imide are strong enough bases to react with the oxides thus rendering them unusable as catalyst supports. (This also implies that the common practice of containing catalyst powders within quartz wool is not a suitable method

for studying amides or imides). By contrast, the evidence from the magnesium oxide reactions with lithium amide and lithium imide suggests that lithium amide under ammonia will only react to form the ternary nitride, which is unstable under ammonia and re-forms the lithium amide. Although the magnesium oxide is not therefore strictly chemically inert to the catalyst, it is potentially suitable as a support since the product of reaction decomposes back to the catalyst itself under ammonia decomposition conditions. This is further confirmed by the unhindered catalytic performance of lithium amide–magnesium oxide mixtures. For all of the potential supports studied there is no enhancement of catalytic performance compared to the lithium amide by itself, which would imply that the supports are only affecting the active sites for ammonia decomposition detrimentally by reaction with the lithium amide, or in the case of magnesium oxide, the re-formation of lithium amide from the addition of ammonia to lithium magnesium nitride re-forms these active sites. Previous isotopic studies of the ammonia decomposition reaction over lithium amide-imide implied that it proceeded via lithium-rich species on the surface of the catalyst.²⁰ Such species are likely to be more basic than lithium amide or imide and therefore the most basic support, magnesium oxide, is the least likely support to interfere with these active, lithium-rich sites.

CONCLUSIONS

Activated carbon, silicon dioxide, aluminium oxide and magnesium oxide were evaluated as potential catalyst supports for the lithium amide-imide ammonia decomposition catalyst, but it was found that all supports displayed some reactivity towards the catalyst itself. In the cases of carbon, silicon dioxide and aluminium oxide this chemical reactivity renders the catalyst unusable and therefore they are inappropriate supports. For magnesium oxide, however, there is formation of a ternary nitride rather than a ternary oxide on reaction with lithium amide-imide. This ternary nitride is unstable in the presence of ammonia and decomposes back to the lithium amide catalyst. As a result, magnesium oxide is potentially a suitable support for the lithium amide-imide catalyst for ammonia decomposition, which is confirmed by the unreduced catalytic performance of the lithium amide with magnesium oxide (in contrast to the other supports). There are still chemical engineering challenges remaining with the use of alkali/alkaline earth metal amide and imide catalysts for ammonia decomposition, however, including the containment of the catalyst and prevention of sintering of catalyst particles.

AUTHOR INFORMATION

Corresponding Author

thomas.wood@stfc.ac.uk

Funding Sources

This work was financially supported by an EPSRC grant “Fuel Cell Technologies for an Ammonia Economy”, EP/M014371/1. JWM would like to thank St John’s College for financial support.

Notes

The authors declare no competing financial interest.

Acknowledgments

The authors acknowledge the technical assistance of James Taylor and Gavin Stenning.

Supporting Information

Includes thermal decomposition mass spectrometry data for: (i) lithium imide under argon; (ii) lithium amide under argon; (iii) lithium amide under ammonia.

REFERENCES

- (1) Green, L., Jr. An ammonia energy vector for the hydrogen economy. *Int. J. Hydrogen Energy* **1982**, *7*, 355–359.
- (2) Klerke, A.; Christensen, C. H.; Nørskov, J. K.; Vegge, T. Ammonia for hydrogen storage: challenges and opportunities. *J. Mater. Chem.* **2008**, *18*, 2304–2310.
- (3) Schüth, F.; Palkovits, R.; Schlögl, R.; Su, D. S. Ammonia as a possible element in an energy infrastructure: catalysts for ammonia decomposition. *Energy Environ. Sci.* **2012**, *5*, 6278–6289.
- (4) “Nitrogen (Fixed)—Ammonia”, U.S. Geological Survey, Mineral Commodity Summaries, 2017.
- (5) Kordesch, K.; Hacker, V.; Gsellmann, J.; Cifrain, M.; Faleschini, G.; Enzinger, P.; Fankhauser, R.; Ortner, M.; Muhr M.; Aronsson, R. R. Alkaline fuel cells applications. *J. Power Sources* **2000**, *86*, 162–165.
- (6) Hunter, H. M. A.; Makepeace, J. W.; Wood, T. J.; Mylius, O. S.; Kibble, M. G.; Nutter, J. B.; Jones, M. O.; David, W. I. F. Demonstrating hydrogen production from ammonia using lithium imide – Powering a small proton exchange membrane fuel cell. *J. Power Sources* **2016**, *329*, 138–147.
- (7) Comotti, M.; Frigo, S. Hydrogen generation system for ammonia—hydrogen fuelled internal combustion engines *Int. J. Hydrogen Energy* **2015**, *40*, 10673–10686.
- (8) Yin, S. F.; Xu, B. Q.; Zhou, X. P.; Au, C. T. A mini-review on ammonia decomposition catalysts for on-site generation of hydrogen for fuel cell applications. *Appl. Catal. A* **2004**, *277*, 1–9.
- (9) Raróg-Pilecka, W.; Szmigiel, D.; Kowalczyk, Z.; Jodzis, S.; Zielinski, J. Ammonia decomposition over the carbon-based ruthenium catalyst promoted with barium or cesium. *J. Catal.* **2003**, *218*, 465–469.
- (10) Hansgen, D. A.; Vlachos, D. G.; Chen, J. G. Using first principles to predict bimetallic catalysts for the ammonia decomposition reaction. *Nat. Chem.* **2010**, *2*, 484–489.
- (11) “Platinum Group Elements”, British Geological Survey, Mineral Profiles, 2009.
- (12) Feyen, M.; Weidenthaler, C.; Güttel, R. Schlicte, K.; Holle, U.; Lu, A.-H.; Schüth, F. High-Temperature Stable, Iron-Based Core–Shell Catalysts for Ammonia Decomposition. *Chem.—Eur. J.* **2011**, *17*, 598–605.
- (13) David, W. I. F.; Makepeace, J. W.; Callear, S. K.; Hunter, H. M. A.; Taylor, J. D.; Wood, T. J.; Jones, M. O. Hydrogen Production from Ammonia Using Sodium Amide. *J. Am. Chem. Soc.* **2014**, *136*, 13082–13085.
- (14) Guo, J.; Wang, P.; Wu, G.; Wu, A.; Hu, D.; Xiong, Z.; Wang, J.; Yu, P.; Chang, F.; Chen, Z.; Chen, P. Lithium Imide Synergy with 3d Transition-Metal Nitrides Leading to Unprecedented Catalytic Activities for Ammonia Decomposition. *Angew. Chem. Int. Ed.* **2015**, *54*, 2950–2954.

- (15) Makepeace, J. W.; Wood, T. J.; Hunter, H. M. A.; Jones, M. O. David, W. I. F. Ammonia decomposition catalysis using non-stoichiometric lithium imide. *Chem. Sci.* **2015**, *6*, 3805–3815.
- (16) Guo, J.; Chang, F.; Wang, P.; Hu, D.; Yu, P.; Wu, G.; Xiong, Z.; Chen, P. Highly Active MnN-Li₂NH Composite Catalyst for Producing CO_x-Free Hydrogen. *ACS Catal.* **2015**, *5*, 2708–2713.
- (17) Makepeace, J. W.; Hunter, H. M. A.; Wood, T. J.; Smith, R. I.; Murray, C. A.; David, W. I. F. Ammonia decomposition catalysis using lithium-calcium imide. *Faraday Discuss.* **2016**, *188*, 525–544.
- (18) Yu, P.; Guo, J.; Liu, L.; Wang, P.; Wu, G.; Chang, F.; Chen, P. Ammonia Decomposition with Manganese Nitride–Calcium Imide Composites as Efficient Catalysts. *ChemSusChem* **2016**, *9*, 364–369.
- (19) Wood, T. J.; Makepeace, J. W.; Hunter, H. M. A.; Jones, M. O.; David, W. I. F. Isotopic studies of the ammonia decomposition reaction mediated by sodium amide. *Phys. Chem. Chem. Phys.* **2015**, *17*, 22999–23006.
- (20) Wood, T. J.; Makepeace, J. W.; David, W. I. F. Isotopic studies of the ammonia decomposition reaction using lithium imide catalyst. *Phys. Chem. Chem. Phys.* **2017**, *19*, 4719–4724.
- (21) David, W. I. F.; Jones, M. O.; Gregory, D. H.; Jewell, C. M.; Johnson, S. R.; Walton, A.; Edwards, P. P. A Mechanism for Non-stoichiometry in the Lithium Amide/Lithium Imide Hydrogen Storage Reaction. *J. Am. Chem. Soc.* **2007**, *129*, 1594–1601.
- (22) Makepeace, J. W.; David, W. I. F. Structural Insights into the Lithium Amide-Imide Solid Solution. *J. Phys. Chem. C* **2017**, *121*, 12010–12017.
- (23) Zhang, J.; Hu, Y. H. Decomposition of Lithium Amide and Lithium Imide with and without Anion Promoter. *Ind. Eng. Chem. Res.* **2011**, *50*, 8058–8064.
- (24) Zhang, J.; Hu, Y. H. Intermediate species and kinetics of lithium imide decomposition. *Int. J. Hydrogen Energy* **2012**, *37*, 10467–10472.
- (25) Pinkerton, F. E. Decomposition kinetics of lithium amide for hydrogen storage materials. *J. Alloys Compd.* **2005**, *400*, 76–82.
- (26) Bramwell, P. L.; Lentink, S.; Ngene, P.; de Jongh, P. E. Effect of Pore Confinement of LiNH₂ on Ammonia Decomposition Catalysis and the Storage of Hydrogen and Ammonia. *J. Phys. Chem. C* **2017**, *120*, 27212–27220.
- (27) Balogh, M. P.; Jones, C. Y.; Herbst, J. F.; Hector, L. G., Jr.; Kundrat, M. Crystal structures and phase transformation of deuterated lithium imide, Li₂ND. *J. Alloys Compd.* **2006**, *420*, 326–336.
- (28) Titherley, A. W. Sodium, Potassium, and Lithium Amides. *J. Chem. Soc.* **1894**, *65*, 504–522.
- (29) Wang, P.; Guo, J.; Xiong, Z.; Wu, G.; Wang, J.; Chen, P. The interactions of Li₃FeN₂ with H₂ and NH₃. *Int. J. Hydrogen Energy* **2016**, *41*, 14171–14177.
- (30) Chen, P.; Xiong, Z.; Luo, J.; Lin, J.; Tan, K. L. Interaction of hydrogen with metal nitrides and imides. *Nature* **2002**, *420*, 302–304.

ToC graphic:

